



# Moisture Absorption and Hydrothermal Aging of Phenylethynyl-Terminated PMDA-Type Asymmetric Polyimide and Composites

Yixiang Zhang<sup>\*,1</sup>, Masahiko Miyauchi<sup>2</sup>, Steven Nutt<sup>1</sup>

<sup>1</sup>Department of Chemical Engineering and Materials Science, University of Southern California, Los Angeles, CA, USA

<sup>2</sup>Kaneka U.S. Material Research Center, Kaneka Americas Holding, College Station, TX, USA

\* E-mail: [zhangyix@usc.edu](mailto:zhangyix@usc.edu)

## ABSTRACT

The effects of moisture on a polymerized monomeric reactant (PMR)-type polyimide (TriA X) and associated composites were investigated. Water uptake tests were performed on the polyimide at various temperatures and relative humidity levels to investigate moisture absorption behavior. Two-stage moisture absorption was observed, in which the first stage was diffusion-controlled, while the second stage was moisture plasticization-controlled. As exposure temperature increased, the equilibrium moisture content of the polyimide decreased, indicating an exothermic absorption process. The Arrhenius temperature dependence and moisture saturation as functions of temperature and humidity in the neat polymer were determined using curve-fitting based on published mathematical models. Long-term hydrothermal aging at 95°C was conducted on the neat polyimide and associated carbon fiber composites. Reversible hydrolytic reactions and a trace of irreversible hydrolysis were observed in the long-term exposure. The tensile ductility of the neat polyimide and the short-beam shear strength of the composites decreased with increasing aging time, while the tensile strength and modulus and thermal properties of the polyimide exhibited little change after 2000-h aging, demonstrating hydrothermal stability. The decrease in the ductility of the neat polymer

Please cite the article as: Zhang, Y., Miyauchi, M., & Nutt, S.. “**Moisture absorption and hydrothermal aging of phenylethynyl-terminated pyromellitic dianhydride-type asymmetric polyimide and composites,**” High Performance Polymers (2018), DOI: [10.1177/0954008318816754](https://doi.org/10.1177/0954008318816754)



after long-term moisture exposure was attributed to the network structure change, driven by hydrolysis and moisture plasticization.

## Keywords

Polyimide, moisture absorption, hydrothermal aging, thermal properties, mechanical properties, plasticization, hydrolysis, composite,  $\beta$ -relaxation

## Introduction

Because of the high transition temperatures ( $T_g$ ) and thermal stability of polyimides, carbon fiber composites with polyimide matrices are deployed in high-service-temperature applications, such as aeroengines and supersonic aircraft.<sup>1, 2</sup> However, polyimide-matrix composites are more expensive than conventional epoxy-matrix composites because of resin costs (200-900 USD kg<sup>-1</sup>) and the complexity of the fabrication/cure process.<sup>3, 4</sup> Thus, long lifetime is expected for polyimide-matrix composites, and stability issues must be addressed before adopting polyimide resins in new engineering applications.

Hydrothermal stability of polyimide systems has been a primary concern for aerospace applications, because polyimides are hydrophilic polymers and thus susceptible to moisture.<sup>5, 6</sup> The general effects of moisture include the hydrolysis of imide units and water plasticization.<sup>5-7</sup> Hydrolysis can depolymerize polyimides by opening imide rings to form polyamic acids, followed by chain scission and regeneration of monomers (or even de-monomerization), resulting in degradation of dry mechanical properties.<sup>5</sup> For example, after 1000-h hydrothermal exposure at 160°C and subsequent drying, one polyimide (AFR700B) manifest ~70% strength loss and ~85% strain-to-failure decrease, while another (K3B) showed ~18% strength loss and a ~21% decrease in strain-to-failure.<sup>5</sup> In addition to chemical reactions, water molecules can act as plasticizing agents in

Please cite the article as: Zhang, Y., Miyauchi, M., & Nutt, S.. **“Moisture absorption and hydrothermal aging of phenylethynyl-terminated pyromellitic dianhydride-type asymmetric polyimide and composites,”** High Performance Polymers (2018), DOI: [10.1177/0954008318816754](https://doi.org/10.1177/0954008318816754)



polymer networks, pushing polymer chains apart, and hence reducing  $T_g$ .<sup>8</sup> This effect, defined as plasticization, can not only reduce  $T_g$  but also adversely affect mechanical properties. For instance, the wet  $T_g$  (256°C) of PMR-15 is 73°C below the dry  $T_g$  (338°C).<sup>9</sup> Because the  $T_g$  decreased sharply with moisture uptake, the wet flexural properties at 260°C and 316°C of HTS-2/PMR-15 composites were 10-20% less than the dry properties at the same temperatures.<sup>10</sup>

Moisture absorption also can lead to permanent damage in polyimide composites. Microcracking is typically the first form of damage to manifest in composites under extended hot/wet exposure.<sup>11</sup> For example, long-term moisture exposure reportedly degraded the “microcracking toughness” of both thermoplastic and thermoset polyimide composites.<sup>12</sup> When the toughness dropped sufficiently, the composites lost ability to withstand internal stresses (generated during manufacturing), and microcracks formed. Microcracking of IM7/K3B and IM7/PETI-5 initiated after water immersion at 80°C for 200 h and 1500 h, respectively.<sup>12</sup> Another type of damage observed in polyimide composites is blistering. When composites are heated, absorbed moisture can vaporize and generate internal pressure. When the vapor pressure exceeds the matrix strength, blistering occurs in the form of macrovoids, microcracks, and/or delamination.<sup>6, 13</sup>

Although the effects of moisture absorption on polyimides and polyimide-matrix composites have been studied for decades, few studies have addressed long-term hydrothermal aging. The present work focuses on both short-term moisture absorption of a new polyimide (TriA X) and the effects of long-term moisture exposure on the neat polymer and associated composites. TriA X is a polymerized monomer reactant (PMR)-type polyimide, derived from pyromellitic dianhydride (PMDA), 2-phenyl-4,4'-diaminodiphenyl ether (p-ODA), and 4-phenylethynyl phthalic anhydride<sup>14</sup>,<sup>15</sup> (PEPA), with a formulated degree of polymerization  $n = 7$  in the imide oligomer.<sup>16</sup> The



asymmetric and nonplanar backbone structure endows the polyimide with exceptional ductility (10-45%) from -54 to 288°C, which surpasses those of conventional polyimides, e.g., PMR-15 and AFR-PE-4.<sup>17</sup> The remarkable ductility of TriA X may expand future high-performance applications of polyimide composites. However, the stability of TriA X is not yet fully investigated. Here, we report the long-term hydrolytic stability of TriA X to further explore the potential of this polyimide as a composite matrix for severe service environments.

Short-term moisture uptake experiments were conducted at different temperatures and relative humidity (RH) to investigate the moisture absorption behavior of neat TriA X. The polyimide exhibited a two-stage, exothermic absorbing process. Moisture uptake models were determined as functions of temperature and moisture. The long-term hydrothermal stability of the neat polyimide and composites were evaluated based on retention of chemical, thermal and mechanical properties. Long-term hydrothermal aging caused no deterioration in thermal properties and negligible permanent chemical degradation. However, ductility decreased with increasing exposure time because of reversible hydrolysis and moisture plasticization, resulting in associated reductions in toughness and short-beam shear (SBS) strength of the associated composites.

## Materials

Neat polyimide panels and films were prepared by molding PMDA *di*-ester/p-ODA/PEPA *mono*-ester powder blend in a hot press.<sup>17</sup> The neat polymer samples were machined to designated sizes for measurements described in the following sections. Polyimide prepreg was fabricated using an 80 wt% PMDA *di*-ester/p-ODA/PEPA *mono*-ester solution in ethanol, which was combined with de-sized T650-35/8HS/3K carbon fabric (areal weight: 368 g m<sup>-2</sup>, Cytac Solvay Group, USA). The prepreg was prepared by calendering the monomer solution on both sides of the fabric. After

Please cite the article as: Zhang, Y., Miyauchi, M., & Nutt, S.. “**Moisture absorption and hydrothermal aging of phenylethynyl-terminated pyromellitic dianhydride-type asymmetric polyimide and composites,**” High Performance Polymers (2018), DOI: [10.1177/0954008318816754](https://doi.org/10.1177/0954008318816754)



fabrication, the prepreg was stored in sealed bags at  $-22^{\circ}\text{C}$  prior to use. T650-35 8HS/polyimide composites were fabricated in two lay-up sequences,  $[0]_8$  and  $[0/+45/-45/90]_s$ , using a molding cycle developed in-house.<sup>16</sup> The composite laminates were machined to  $18\times6\times3$  mm specimens for SBS tests.

## Experiments

### *Short-term moisture uptake*

The moisture diffusion behavior was investigated by short-term water uptake of neat polyimide specimens ( $70.0\times12.7\times3.1$  mm) at  $35^{\circ}\text{C}$ ,  $55^{\circ}\text{C}$ ,  $75^{\circ}\text{C}$  and  $95^{\circ}\text{C}$ . Prior to absorption experiments, the samples were dried at  $95^{\circ}\text{C}$  for 94 h and then at  $151^{\circ}\text{C}$  for 92 h under vacuum until the weight stabilized. Next, specimens were immersed in deionized water at different temperatures, and the weight change was monitored as a function of time. The water temperature was controlled by a digital heating controller (MC810, Electrothermal, UK). At each temperature, five specimens were tested, and all specimens were machined from the same panel.

The relationship between maximum moisture content and ambient relative humidity was determined by conditioning neat polyimide specimens ( $70.0\times12.7\times3.1$  mm) at different humidity levels created from selected saturated salt solutions.<sup>18</sup> Saturation was performed in sealed containers with saturated  $\text{MgCl}_2$  (38.5% RH),  $\text{NaBr}$  (54.0% RH) and  $\text{NaCl}$  (77.0% RH) solutions, respectively, at  $35^{\circ}\text{C}$ . Humidity and temperature were recorded using stand-alone data loggers (EL-USB-2, Lascar Electronics, UK). Prior to moisture exposure, all samples were dried using the method described above. At each relative humidity, five specimens were tested.

### *Long-term hydrothermal aging*

Please cite the article as: Zhang, Y., Miyauchi, M., & Nutt, S.. “**Moisture absorption and hydrothermal aging of phenylethynyl-terminated pyromellitic dianhydride-type asymmetric polyimide and composites,**” High Performance Polymers (2018), DOI: [10.1177/0954008318816754](https://doi.org/10.1177/0954008318816754)



Long-term hydrothermal aging tests at 95°C were conducted to investigate the effects of moisture absorption on the properties of the neat polymer and associated composites. The long-term water uptake was performed by immersing the specimens (as machined) in a hot water bath at 95°C. The specimens were removed from the water bath every 1000 h for property measurements in dry and wet conditions. Prior to dry tests, the unaged and aged specimens were dried at 95°C under vacuum for 3 days, then stored in a desiccator at room temperature for at least 4 days, while the aged specimens for wet tests were stored in a water bath at room temperature prior to testing. The unaged wet specimens were water-conditioned at room temperature until saturation was reached.

#### *Fourier-transform infrared spectroscopy*

Attenuated total reflectance Fourier transform infrared spectroscopic analysis (ATR-FTIR; Nicolet 4700, Thermo Fisher Scientific, USA) was performed to investigate the chemical structure change during long-term hydrothermal aging. The spectra were recorded by scanning the neat polymer films (~0.1 mm thick) with a diamond single bounce ATR sampling accessory (Smart Orbit, Thermo Fisher Scientific, USA). 128 scans were performed for each sample.

#### *X-ray photoelectron spectroscopy*

The surface chemistry of polyimide films before and after long-term aging was analyzed using an X-ray photoelectron spectrometer (XPS; Kratos AXIS Ultra, Kratos Analytical, UK). The instrument featured a monochromatic Al K $\alpha$  source (1486.6 eV) at 3 mA and 6 kV. Survey spectra were acquired at 160 eV pass energy with 1 eV step, followed by narrow region spectra (O 1s, N 1s and C 1s) acquired at 40 eV pass energy with 0.1 eV step. 5 sweeps were conducted for survey spectra and 15 sweeps for each element range. The operating pressure was  $\sim 1 \times 10^{-9}$  Torr, so XPS



was performed only on dry specimens. Four different locations were scanned on each sample, and spectra were analyzed using software (CasaXPS version 2.3.16, Casa Software Ltd., UK).

### *Dynamic mechanical analysis*

Dynamic mechanical analysis (DMA) was performed on both the dry and wet neat polyimide specimens to determine the  $T_g$  values and structural relaxations before and after hydrothermal aging (Q800, TA Instruments, USA). Measurements were performed in single cantilever mode at a heating rate of  $5^{\circ}\text{C min}^{-1}$  with a fixed frequency of 1 Hz and a strain of 0.3%. The temperature range for each measurement was  $-90^{\circ}\text{C}$ - $450^{\circ}\text{C}$ , achieved using a gas cooling accessory (Q Series<sup>TM</sup>, TA Instruments, USA).  $T_g$  was determined by  $\tan \delta$  maximum.

### *Thermogravimetric analysis*

Thermogravimetric analysis (TGA) of polyimide samples was performed under nitrogen purge at a flow rate of  $25.00 \text{ ml min}^{-1}$  (Q5000, TA Instruments, USA). TGA data were acquired to determine the decomposition temperature after every 1000-h hydrothermal aging at  $95^{\circ}\text{C}$ . TGA was performed on dry polyimide films only. To remove residual moisture, the films were dried at  $100^{\circ}\text{C}$  for 1 h in the TGA, prior to each measurement. Subsequently, the films were heated from  $30^{\circ}\text{C}$  to  $600^{\circ}\text{C}$  at a rate of  $10^{\circ}\text{C min}^{-1}$ . The decomposition temperature was defined as the temperature of 5% weight loss ( $T_{d5\%}$ ).

### *Tensile tests*

The effects of hydrothermal aging on tensile properties of the neat polyimide were measured in accordance with ASTM D638 standard.<sup>19</sup> Dimension, condition, and number of specimens are given in Table 1. The tests were conducted using a load frame (5567, Instron, USA) with a 5000-N load cell (2525-805, Instron, USA). Tensile tests were performed at a displacement rate of  $1.0 \text{ mm min}^{-1}$

Please cite the article as: Zhang, Y., Miyauchi, M., & Nutt, S.. “**Moisture absorption and hydrothermal aging of phenylethynyl-terminated pyromellitic dianhydride-type asymmetric polyimide and composites,**” High Performance Polymers (2018), DOI: [10.1177/0954008318816754](https://doi.org/10.1177/0954008318816754)



at room temperature. The strain was measured using a 3-D optical displacement measuring system (ARAMIS; Adjustable Base 2.3 M, GOM, Germany). Speckle patterns were painted on the gauge sections of the specimens prior to the tests. As the specimens deformed, the measuring system tracked the speckle pattern evolution to determine dimension change.

Table 1. Specimens for tensile tests.

Aging time (h)	Condition	Length <sup>a</sup> (mm)	Width <sup>b</sup> (mm)	Thickness <sup>b</sup> (mm)	Number of specimens
0	Dry	66.0	3.16	3.13	6 <sup>c</sup>
	Wet	66.0	3.19	3.12	6
1000	Dry	66.0	3.18	3.09	5
	Wet	66.0	3.17	3.12	5
2000	Dry	66.0	3.15	3.08	5
	Wet	66.0	3.20	3.11	5

<sup>a</sup>Total length of specimens.

<sup>b</sup>Gauge section dimensions.

<sup>c</sup>The test results are taken from previous work.<sup>17</sup>

### *Short-beam shear tests*

The SBS strength of T650-35 8HS composites was measured at room temperature in accordance with ASTM D2344 standard.<sup>20</sup> Dimension, condition, lay-up sequence, and number of specimens are summarized in Table 2. The tests were performed on a load frame at a crosshead displacement rate of 1.0 mm min<sup>-1</sup> with a support span of 12.5 mm for all specimens.

Table 2. Specimens for SBS tests.

Please cite the article as: Zhang, Y., Miyauchi, M., & Nutt, S.. “**Moisture absorption and hydrothermal aging of phenylethynyl-terminated pyromellitic dianhydride-type asymmetric polyimide and composites,**” High Performance Polymers (2018), DOI: [10.1177/0954008318816754](https://doi.org/10.1177/0954008318816754)





Lay-up sequence	Aging time (h)	Condition	Length (mm)	Width (mm)	Thickness (mm)	Number of specimens
[0] <sub>8</sub>	0	Dry	18.41	6.13	3.08	5
		Wet	18.44	6.13	3.07	7
	1000	Dry	18.44	6.13	3.11	5
		Wet	18.43	6.11	3.09	5
	2000	Dry	18.44	6.14	3.09	6
		Wet	18.45	6.13	3.12	5
[0/+45/-45/90] <sub>s</sub>	0	Dry	18.64	6.20	3.10	8
		Wet	18.66	6.21	3.12	7
	1000	Dry	18.64	6.21	3.12	5
		Wet	18.66	6.19	3.10	5
	2000	Dry	18.67	6.22	3.09	7
		Wet	18.69	6.23	3.13	6

## Results and discussion

### *Moisture absorption behavior*

The moisture content ( $M_t$ ) of neat TriA X is plotted as a function of water immersion time at different temperatures in Figure 1. The moisture content is defined by

$$M_t = \frac{W_{wet} - W_{dry}}{W_{dry}} \times 100\% \quad (1)$$

where  $W_{wet}$  is the wet sample weight, and  $W_{dry}$  is the dry sample weight. The symbols in Figure 1 are the measured values. In the initial stage of water absorption, Fickian diffusion behavior was observed, i.e., the moisture content was linearly proportional to the square root of time. However,

Please cite the article as: Zhang, Y., Miyauchi, M., & Nutt, S.. “**Moisture absorption and hydrothermal aging of phenylethynyl-terminated pyromellitic dianhydride-type asymmetric polyimide and composites,**” High Performance Polymers (2018), DOI: [10.1177/0954008318816754](https://doi.org/10.1177/0954008318816754)



after the moisture absorption reached a near-equilibrium stage (plateaus in Figure 1), the moisture content continued to increase, albeit at a much slower rate compared to the initial stage. The observed moisture absorption behavior conforms to the two-stage diffusion model reported by Bao et al for a bismaleimide polymer.<sup>7</sup> The first stage is diffusion-controlled, while the second stage is governed by network relaxation induced by moisture plasticization, where the absorbed water molecules create swelling that opens the structural network and renders it more accessible to additional moisture. This two-stage diffusion model is described by<sup>7</sup>

$$M_t = M_{\infty 0} (1 + k\sqrt{t}) \left\{ 1 - \exp \left[ -7.3 \left( \frac{Dt}{h^2} \right)^{0.75} \right] \right\} \quad (2)$$

where  $M_{\infty 0}$  is the moisture content (quasi-equilibrium) at the end of the Fickian diffusion,  $k$  characterizes the relaxation rate in the second stage,  $t$  is moisture absorbing time,  $D$  is diffusivity, and  $h$  is specimen thickness.

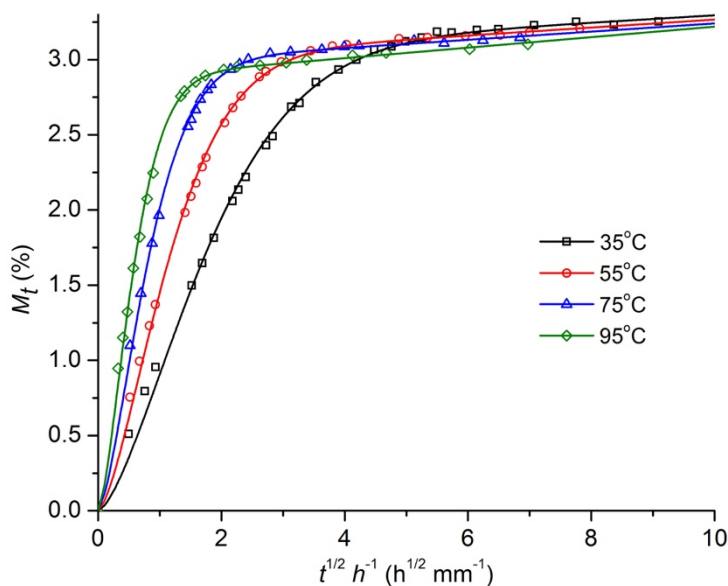


Figure 1. Moisture gain of neat polyimide in water at different temperatures. The symbols are experimental values, and the solid lines are curve fits using Equation (2).

Please cite the article as: Zhang, Y., Miyauchi, M., & Nutt, S.. “**Moisture absorption and hydrothermal aging of phenylethynyl-terminated pyromellitic dianhydride-type asymmetric polyimide and composites,**” High Performance Polymers (2018), DOI: [10.1177/0954008318816754](https://doi.org/10.1177/0954008318816754)



Because of the low surface-to-edge areal ratio (7:2), the diffusion through the edges of the specimens cannot be neglected, and edge correction must be considered when using Equation (2) to determine diffusivity. In Equation (2),  $D$  is the apparent diffusivity determined from diffusion through all six surfaces in three directions. Because the neat polymer is an isotropic and homogeneous material, the diffusivities in all three directions are equal. The true one-directional diffusivity  $D_x$  is given by<sup>21</sup>

$$D_x = D \left( 1 + \frac{h}{l} + \frac{h}{n} \right)^{-2} \quad (3)$$

where  $l$  and  $n$  are the length and width of specimens. The diffusivity values at different temperatures were determined by curving-fitting the experimental results using Equation (2). The fitting results are summarized in Table 3, and the fitting curves are plotted in Figure 1 as solid lines. All fits yield  $R^2 > 0.99$ , indicating accurate fitting.

Table 3. Curve fitting results using Equation (2) and (3).

Temperature (°C)	$M_{\infty 0}$ (%)	$k$ ( $10^{-5}$ % $s^{-1/2}$ )	$D$ ( $10^{-6}$ mm <sup>2</sup> s <sup>-1</sup> )	$D_x$ ( $10^{-6}$ mm <sup>2</sup> s <sup>-1</sup> )
35	3.04±0.02	4.42±0.22	4.82±0.07	2.89±0.05
55	2.97±0.02	4.67±0.20	10.76±0.23	6.51±0.04
75	2.97±0.01	4.95±0.15	22.38±0.29	13.58±0.11
95	2.90±0.02	6.23±0.22	44.74±0.44	26.92±0.40

The diffusivity increased with temperature. Plotting  $\ln(D_x)$  as a function of  $1/T$  yielded a linear relationship (solid black line in Figure 3) consistent with the Arrhenius equation:

$$D_x = D_{x0} \exp \left( -\frac{E_a}{RT} \right) \quad (4)$$



where  $R$  is the gas constant, and the activation energy ( $E_a$ ) and pre-exponential factor ( $D_{x0}$ ) were determined by the slope and intercept of the Arrhenius plot. Note that the moisture saturation ( $M_\infty$ ) values (shown in Figure 1) decreased as exposure temperature increased, indicating an exothermic moisture absorption process. The moisture saturation and heat of absorption ( $\Delta H$ ) also followed an Arrhenius relationship:<sup>22</sup>

$$M_\infty = M_0 \exp\left(-\frac{\Delta H}{RT}\right) \quad (5)$$

where  $M_0$  is a pre-exponential factor.  $M_0$  and  $\Delta H$  values were calculated using two methods. In Method I,  $M_0$  and  $\Delta H$  were determined directly from the Arrhenius plot of experimental  $M_\infty$  values (blue dashed line in Figure 2). In Method II, we applied the equation:<sup>23</sup>

$$\ln\left(\frac{dM_t}{d\sqrt{t}/h}\right) = \ln\left(4M_0\sqrt{\frac{D_0}{\pi}}\right) - \frac{\frac{E_a}{2} + \Delta H}{RT} \quad (6)$$

where  $dM_t/d\sqrt{t}/h$  is the initial moisture absorbing rate that was determined by the slope of the initial linear part in Figure 1, and  $D_0$  is the pre-exponential factor of the Arrhenius equation of the apparent diffusivity, which was calculated using the method used for determining  $D_{x0}$ . The Arrhenius temperature dependence of  $M_\infty$ , determined using Equation (6), is plotted in Figure 2 (dash-dot blue line). All calculated values as described above are summarized in Table 4.

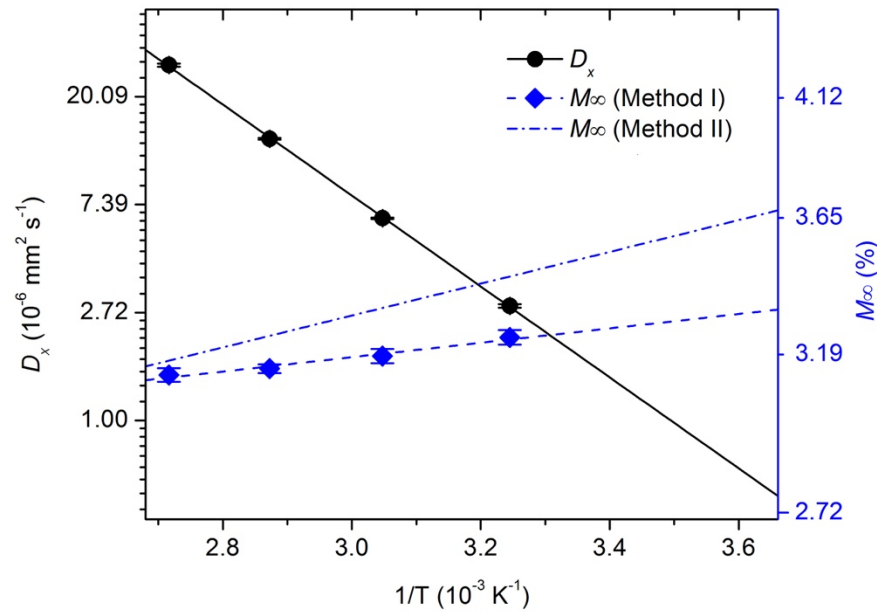


Figure 2. Diffusivity and moisture saturation in water vs  $1/T$ . The black circle symbols are  $D_x$  listed in Table 3, and the blue diamond symbols are experimental results of  $M_\infty$ . The black solid line is curve fit using Equation (4), and the blue dashed and dot-dash lines are curve fits by Methods I and II, respectively.

Table 4. Arrhenius parameters of Equation (4) and (5).

$D_{x0} \text{ (} 10^{-6} \text{ mm}^2 \text{ s}^{-1}\text{)}$	2.49
$D_0 \text{ (} 10^{-6} \text{ mm}^2 \text{ s}^{-1}\text{)}$	4.03
$E_a \text{ (kJ/mol)}$	35.0
$M_0 \text{ (Method I) (%)}$	2.56
$\Delta H \text{ (Method I) (kJ/mol)}$	-0.60
$M_0 \text{ (Method II) (%)}$	2.05
$\Delta H \text{ (Method II) (kJ/mol)}$	-1.33

As shown in Figure 2, Method II overpredicts  $M_\infty$ , yielding values 1-10 % greater than those from Method I (from 0°C to 100°C). Using Method I, we assume no moisture in the specimens prior to moisture exposure. However, the specimens were wet-machined, and it is difficult to remove all moisture from polyimides, because a small portion of water molecules are strongly bonded.<sup>6, 7</sup> On Please cite the article as: Zhang, Y., Miyauchi, M., & Nutt, S.. “**Moisture absorption and hydrothermal aging of phenylethynyl-terminated pyromellitic dianhydride-type asymmetric polyimide and composites,**” High Performance Polymers (2018), DOI: [10.1177/0954008318816754](https://doi.org/10.1177/0954008318816754)



the other hand, despite the presence of residual moisture, the initial absorbing rate ( $dM_t/d\sqrt{t}/h$ ) was controlled by temperature. Therefore, the Arrhenius parameters determined by Method II are considered more accurate.

Conditioning at different relative humidity levels was performed on neat polymer samples to determine the relationship between maximum moisture content and the ambient humidity. The moisture saturation of neat polymer as a function of relative humidity ( $\phi$ ) is shown in Figure 3 and described by<sup>21</sup>

$$M_{\infty} = a\phi^b \quad (7)$$

where  $a$  and  $b$  are constants. In Equation (7),  $a = 0.0059$  and  $b = 1.4$  were determined by curve fitting experimental results (black circles in Figure 3). The fitting yielded a  $R^2 > 0.99$ .

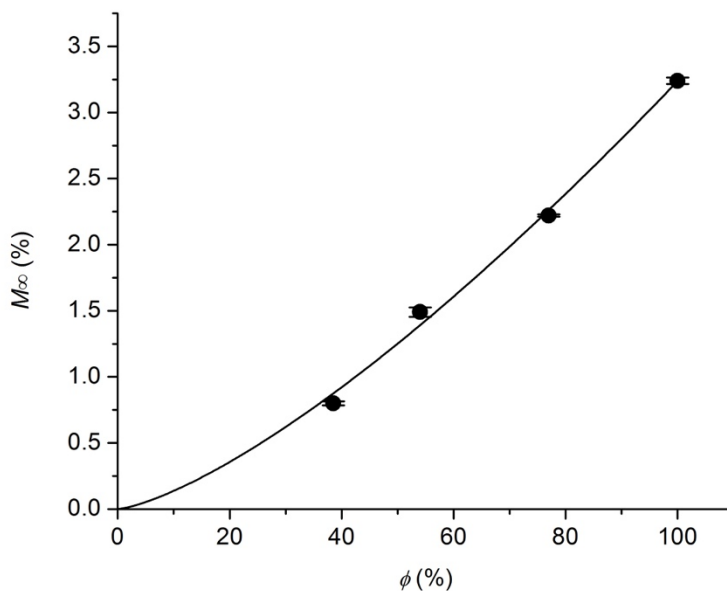


Figure 3. Moisture saturation vs relative humidity at 35°C.

The measured moisture absorption behavior yields a clearer understanding of TriA X and how it is likely to behave in service. Equation (5) or (6) for  $M_{\infty}$  describes the maximum moisture content at a given temperature under 100% RH. However, moisture saturation of polymers is more sensitive

Please cite the article as: Zhang, Y., Miyauchi, M., & Nutt, S.. “**Moisture absorption and hydrothermal aging of phenylethynyl-terminated pyromellitic dianhydride-type asymmetric polyimide and composites,**” High Performance Polymers (2018), DOI: [10.1177/0954008318816754](https://doi.org/10.1177/0954008318816754)



to humidity than to temperature.<sup>21</sup> Although the relationship described by Equation (7) was determined at room temperature (35°C), the relation has practical significance. Relative humidity in a given circumstance is readily measured, so Equation (7) can be used as a predictive tool to estimate moisture content of polyimide components in the field. Moreover, understanding the moisture absorption behavior is essential when addressing issues governed by moisture diffusion kinetics. For instance, the Arrhenius parameters of diffusion are critical for prediction of moisture-induced damage, such as blistering<sup>13</sup> and microcracking<sup>12</sup>, using existing mathematical models.

### *Hydrothermal aging*

#### *Hydrolysis*

Both reversible and irreversible hydrolysis of imide units were detected after extended hydrothermal aging of the neat polymer. The FTIR spectra before and after hot/wet exposure are shown in Figure 4. To examine the reversibility of chemical changes upon absorption or desorption, FTIR was performed on both dry and wet specimens. After 2000-h aging at 95°C, the spectra remained nearly identical to those acquired before exposure when comparing either the dry or wet sets only. However, the intensity of the peak at 1601 cm<sup>-1</sup> was greater in the wet spectra (blue and red curves in Figure 4). This peak corresponds to N-H deformation in amides and/or amines.<sup>23</sup> The greater intensity of the peak in the wet spectra indicates hydrolysis of the imide rings upon water absorption (Figure 5). After moisture desorption, the intensity decreased to the original level in the dry spectra (green and black curves in Figure 4), providing evidence that the hydrolysis is reversible. However, the FTIR results did not exclude the possibility of irreversible hydrolysis upon hot/wet exposure.

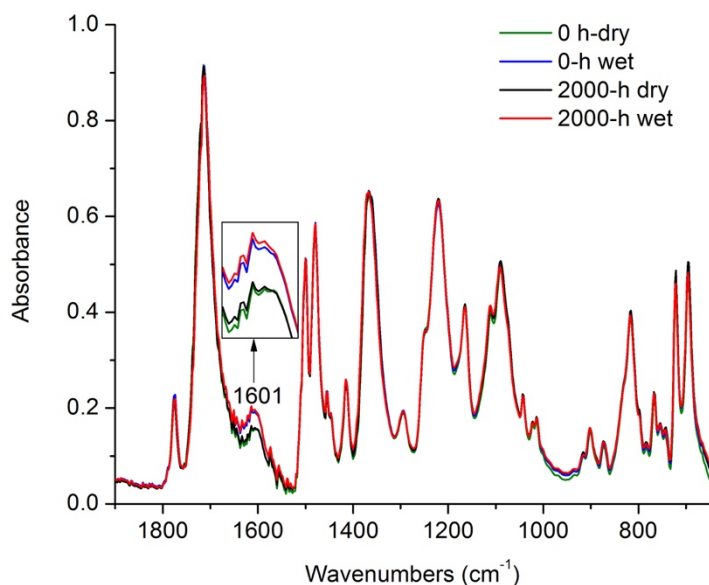


Figure 4. FTIR spectra of TriA X.

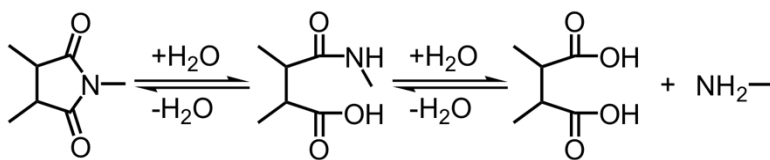


Figure 5. Hydrolytic reactions in polyimides.

XPS analysis was performed on dry specimens before and after hydrothermal aging to measure the composition change. After 2000-h hydrothermal aging and subsequent drying, the O/C mole ratio increased from  $0.154 \pm 0.006$  (dry fresh polymer) to  $0.162 \pm 0.007$  (5.2% increase), indicating moisture remaining in the polymer network in the form of hydrolytic products. The extent of irreversible hydrolysis was small compared to the reversible reaction, because no change was detected in the dry FTIR spectrum after 2000-h aging, but the irreversible hydrolysis might affect the physical properties of the polymer, discussed next.

### *Thermal properties*





The  $\tan \delta$  curves before and after hydrothermal aging are shown in Figure 6. Two major transitions in terms of  $\tan \delta$  maxima were observed in the measured temperature range (-90°C-450°C), labeled  $\alpha$  and  $\beta$  in decreasing order of temperature in accordance with conventional nomenclature.<sup>24</sup> Because of the difference in the magnitudes of  $\alpha$  and  $\beta$  transitions, the  $\tan \delta$  curves are shown in two temperature ranges (-90°C-300°C in Figure 6a and 200°C-300°C in Figure 6b) to present the complete curve shape for each transition.  $\alpha$ -relaxation represented the glass transition and corresponded to the onset of long-range mainchain motion (Figure 6b).  $\beta$ -relaxation was a secondary transition below  $T_g$  in amorphous polymers – a relaxation process active in the glassy state.<sup>8</sup> Various types of motion, such as motions of side groups, restricted motion of the main chain, or motions of end groups, can contribute to the  $\beta$ -transition.<sup>24</sup> Thus, changes in polymer network structure are manifest through  $\beta$ -relaxation, which is sensitive to physical aging.<sup>7, 25</sup> The wet  $\alpha$ -peaks (dashed lines in Figure 6b) were broader than the dry  $\alpha$ -peaks (solid lines in Figure 6b), indicating greater heterogeneity<sup>26</sup> in the wet polymers resulting from the hydrolysis. Meanwhile, the wet  $\alpha$ -peaks shifted slightly (2°C) towards lower temperatures, which can be attributed to both the hydrolytic reactions and to water plasticization effects on the polymer network. The  $\alpha$ -peaks after long-term aging (blue and red lines) were slightly broader than the fresh peaks (black lines in either wet or dry tests, indicating (1) increasing extent of hydrolysis with exposure time and (2) the presence of permanent hydrolytic degradation after long-term exposure and subsequent desorption.

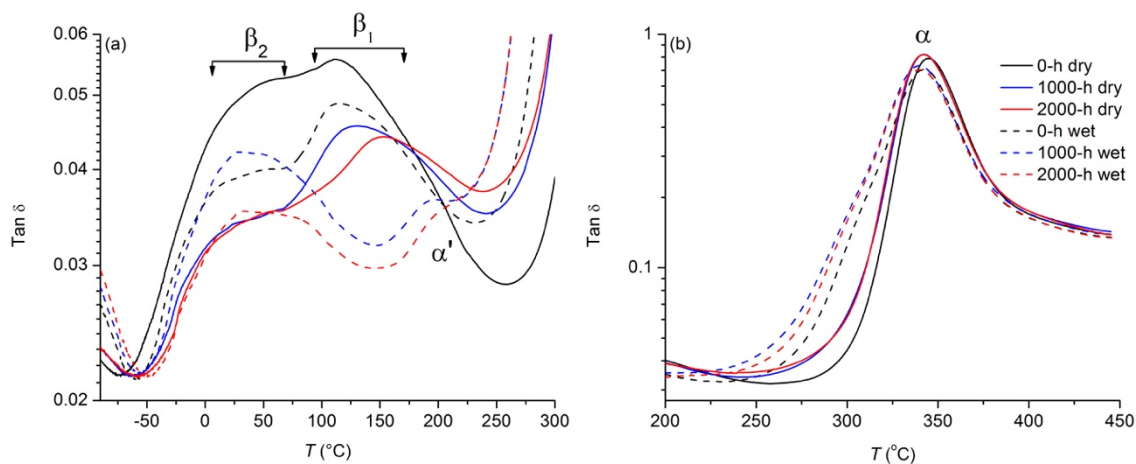


Figure 6. Tan  $\delta$  curves of TriA X.

$\beta$ -relaxation of neat TriA X split into two peaks, labelled  $\beta_1$  (30-50°C) and  $\beta_2$  (110-150°C) in Figure 6a. This split demonstrates the inhomogeneity in the network.  $\beta_1$ -peaks were presented in the tan  $\delta$  curves for both the dry specimens (solid curves) and the wet fresh specimen (black dashed curve). However, after long-term aging, the  $\beta_1$ -peaks disappeared in the tan  $\delta$  curves of the wet specimens, while the  $\alpha$ -transition split, forming a small peak at ~200°C labeled  $\alpha'$  (blue and red dashed lines in Figure 6a). This change indicates that the short-range molecular motions in  $\beta_1$ -relaxation were converted into longer-range motions responsible for the  $\alpha'$ -peaks. Although the mechanism of the structural change is not fully understood, the reversible hydrolytic reactions were clearly responsible for this conversion, because  $\beta_1$ -relaxation reoccurred after moisture desorption, while  $\alpha'$ -peaks were absent. Despite that change in magnitude,  $\beta_2$ -relaxation exhibited only a minor influence from the hydrolytic reactions. The interpretation of the transitions in tan  $\delta$  curves can be useful as a tool to identify physical/chemical reactions induced by environmental exposure, as well as the resulting change in polymer structure, which could influence other properties, e.g., mechanical properties, as discussed in the next section.

Please cite the article as: Zhang, Y., Miyauchi, M., & Nutt, S.. “**Moisture absorption and hydrothermal aging of phenylethynyl-terminated pyromellitic dianhydride-type asymmetric polyimide and composites,**” High Performance Polymers (2018), DOI: [10.1177/0954008318816754](https://doi.org/10.1177/0954008318816754)



The  $T_g$  (peak of  $\alpha$  transition) and  $T_{d5\%}$  values of the neat polymer are shown in Figure 7 ( $T_{d5\%}$  = temperature of 5% weight loss). The  $T_{d5\%}$  value was unchanged after aging, while the wet  $T_g$ 's exhibited negligible reduction (0.6%) compared to the corresponding dry values, and after 2000-h aging, the decrease in both dry and wet  $T_g$  was negligible (0.6%). The nearly 100% retention of  $T_g$  upon moisture exposure is notable. In contrast, the effects of moisture plasticization and hydrolysis on conventional polyimides (e.g. PMR-15, PETI-5, K3B, AFR-700B, *etc*) are typically much greater, with 15-20% reduction in the wet  $T_g$ 's relative to the dry  $T_g$  values.<sup>5, 9, 27</sup> Moreover, significant permanent hydrolytic degradation of imide units has been reported in water uptake studies below 100°C, which can cause a permanent decrease in  $T_g$ .<sup>5, 23</sup>

The effects of plasticization depend on the physical structure of a polymer. The TriA X polyimide features an asymmetric/nonplanar backbone structure. The pendent phenyl group hinders rotation of the diphenyl ether linkage in the ODA moiety, raising the internal rotation energy barrier of the backbone, increasing the chain stiffness. Although the absorbed water molecules generated swelling stress and tended to make the polymer network more open, the rigid polymer chains retarded the structure relaxation process, as evidenced by the nearly flat slope of the second absorption stage in Figure 1. Even after moisture saturation, the stiff chains continued to dominate the  $T_g$ . On the other hand, the ~100% retention of  $T_g$  upon moisture exposure indirectly demonstrated the degree of depolymerization in hydrolysis. Chain scissions (the second reaction in Figure 5) were unlikely to participate in the hydrolysis of TriA X, because chain scissions would cause a more significant  $T_g$  knockdown.<sup>5</sup> Thus, polyamic acid linkages were the major hydrolytic products in the hydrolysis of imide rings (the first reaction in Figure 5). Meanwhile, given the negligible  $T_g$  decrease, the formation of polyamic acid linkages was less than 30-40%.<sup>6</sup>

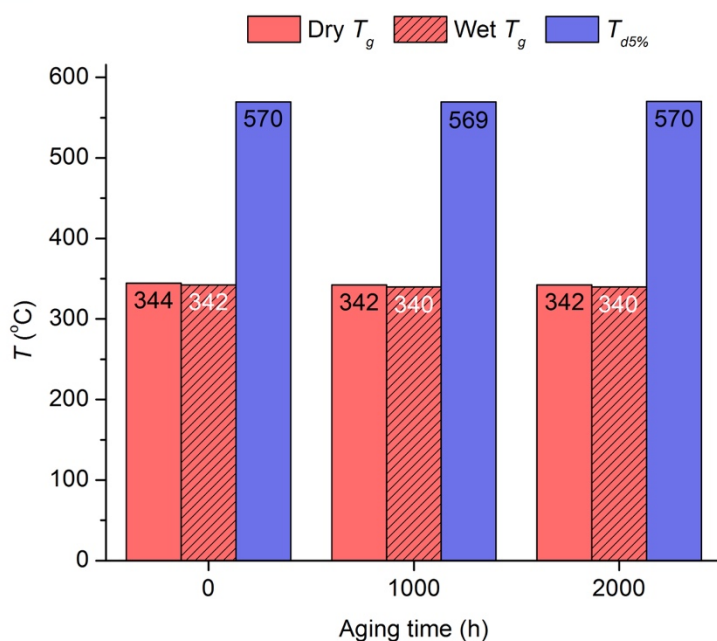


Figure 7.  $T_g$  and  $T_{d5\%}$  of TriA X.

### *Mechanical behavior*

Mechanical tests were performed on neat polymer and composites at room temperature, both before and after moisture exposure, and the tensile properties are summarized in Figure 8. Tensile modulus exhibited no change upon hot/wet exposure. In tests of the fresh polymer, wet specimens exhibited 1% lower strength, but 28% greater strain-to-failure than the dry specimens. The increased ductility translated to 30% greater toughness. Toughness, the energy absorbed during loading prior to failure, was determined from the area under the tensile strain-stress curve.<sup>8</sup> The tougher mechanical response of the wet polymer is consistent with the moisture plasticization effects,<sup>28</sup> in that the absorbed moisture effectively acted as a lubricant, easing the movement of the polymer chains and pushing them further apart.<sup>8</sup> After 2000 h of hot/wet exposure, the dry strength increased by 5%, while the wet strength decreased by 4% relative to the fresh group. In contrast, the dry and wet ductility dropped by 29% and 51%, respectively, after 2000-h aging. These decrements led to



corresponding reductions in the dry and wet toughness of 27% and 56%, respectively. After long-term aging, the difference between the dry and wet toughness was less significant than that in the fresh group, indicating that hydrolysis might have affected the mechanical behavior. Thus, the 9% reduction in wet strength after 2000-h aging was attributed to both reversible hydrolytic reactions and to moisture plasticization.

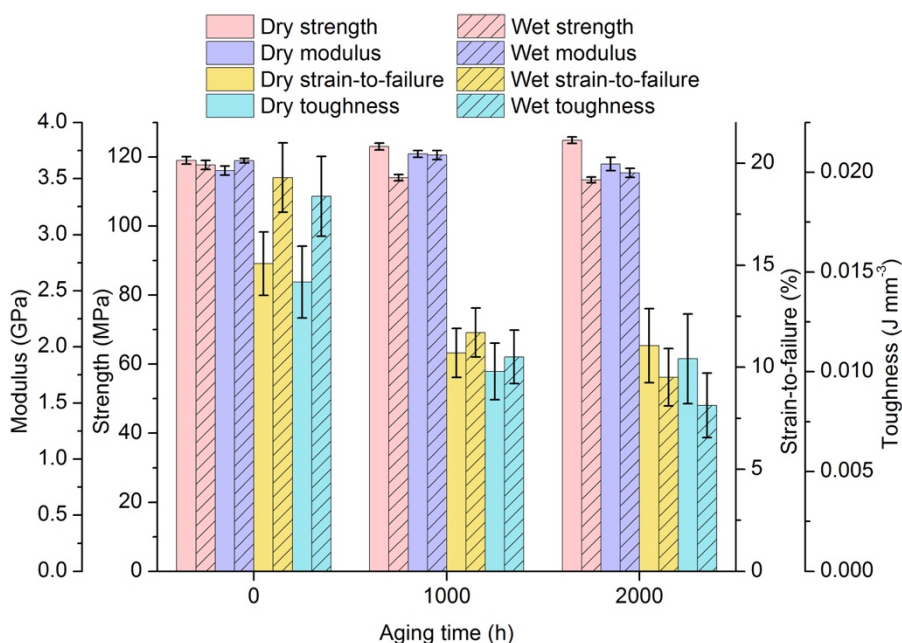


Figure 8. Tensile properties of neat polymer (TriA X).

The decrease in dry/wet toughness and ductility upon aging can be attributed to the change in  $\beta$ -relaxation. The stress-strain curves (Figure 9) of the 2000-h group were nearly identical to those of the 1000-h group except for a slight difference (9-19%) in strain-to-failure, which was attributed to normal measurement variance, given the large scatter of the measured values. This phenomenon indicated that mechanical properties had stabilized before or at 1000 h. Similar stabilization was also observed in the  $\tan \delta$  curves, where the peak positions of the transitions exhibited only minor change



after 1000-h aging (Figure 6). This stabilization indirectly supports a connection between mechanical properties and  $\beta$ -relaxation. Johari indicated that the  $\beta$ -relaxation process in a mechanically rigid glass can be attributed to loosely packed regions with high mobility.<sup>29</sup> Such highly mobile regions would also contribute to the chain motion in mechanical behavior. After long-term aging, the decreased area of  $\beta$ -relaxation, especially  $\beta_1$ -peaks (Figure 6a), indicated that loosely packed regions were at least partially consumed, resulting in segments or groups that were less mechanically active. This network structure change can be attributed to hydrolysis and plasticization. Bao et al indicated that the structural change in bismaleimide polymers induced by moisture absorption is irreversible.<sup>7</sup> Such irreversible structural change is consistent with the observation that neither ductility nor toughness were recovered after drying, although the details of the moisture-induced physical structure change are not yet fully understood. More investigation is required to identify the groups and/or motions that were altered by moisture absorption, and how such changes affect mechanical properties.

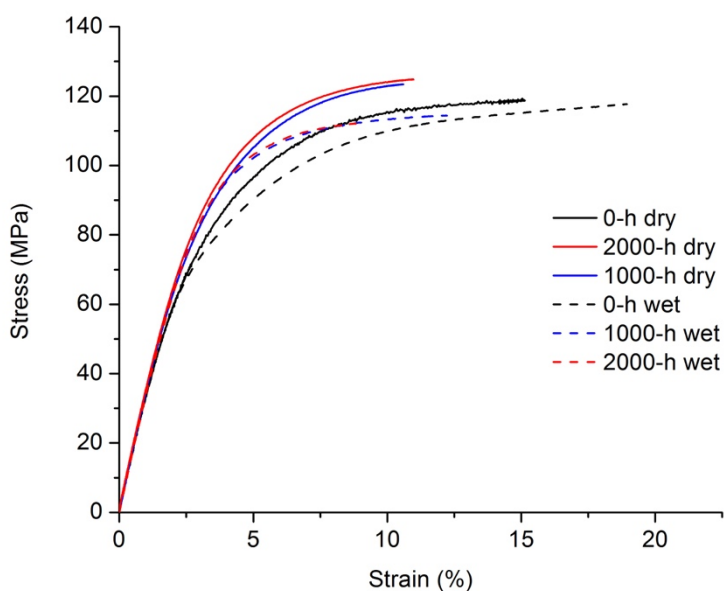


Figure 9. Stress-stain curves of TriA X in tensile tests.

Please cite the article as: Zhang, Y., Miyauchi, M., & Nutt, S.. “**Moisture absorption and hydrothermal aging of phenylethynyl-terminated pyromellitic dianhydride-type asymmetric polyimide and composites,**” High Performance Polymers (2018), DOI: [10.1177/0954008318816754](https://doi.org/10.1177/0954008318816754)



The effects of hydrothermal aging on composites are matrix- and interface-dominated, because only the matrix absorbs moisture, and matrix degradation occurs primarily along matrix-fiber interfaces.<sup>11, 30</sup> Matrix- and interface-dominated mechanical properties are expected to be more affected by moisture than fiber-dominated properties, and SBS strength is good example of an matrix- and interface-dominated property.<sup>31</sup> Thus, SBS strength was selected to characterize the change of the mechanical performance of T650-35 8HS/TriA X composites upon moisture exposure. After 2000-h moisture exposure, the SBS strength decreased by 7-13%, and also in most cases (except the unaged [0/+45/-45/90]<sub>s</sub> group), the wet SBS strength was 1-6% greater than the dry strength (Figure 10). The slight reduction in SBS strength of the composites was attributed to the decrease in matrix toughness, as discussed above. The slightly (2-5%) greater SBS strength retention observed in the aged [0]<sub>8</sub> laminates compared to [0/+45/-45/90]<sub>s</sub> laminates was attributed to effects of lay-up sequences – the SBS strength of quasi-isotropic lay-ups is more matrix-controlled than that of cross-ply lay-ups.<sup>32</sup>

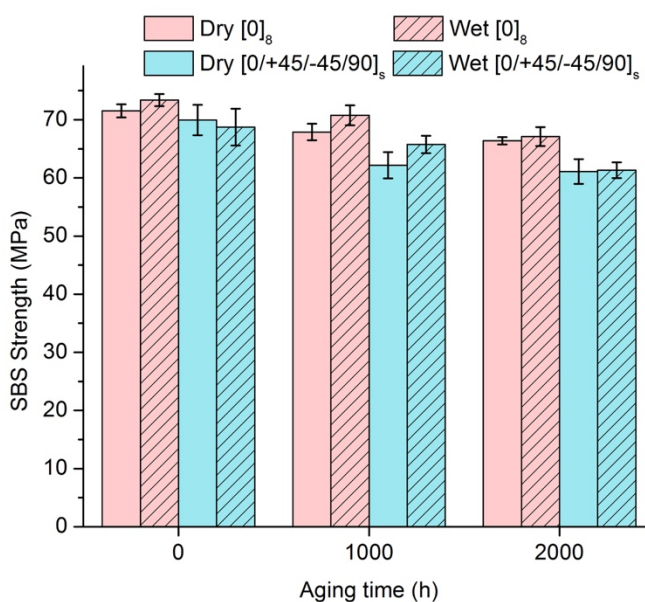






Figure 10. SBS strength of T650-35 8HS/TriA X composites.

## Conclusions

The effects of moisture on a new polyimide – TriA X – were investigated to understand the stability of this polymer in potential high-temperature service environments. Short-term water uptake study at different temperature and relative humidity was performed to gain an accurate understanding of the moisture absorption behavior of the neat polymer. The polyimide exhibited a two-stage moisture diffusion behavior, where the first stage was Fickian diffusion-controlled, while the second stage was governed by the moisture plasticization. Mathematical models of moisture uptake as functions of temperature and humidity were determined and compared to measured behavior. Such models can be used as tools to estimate the moisture content of a component fabricated with the polyimide in the field. More importantly, this work built a foundation for future study on moisture-induced damage in composites, because the Arrhenius parameters determined here are essential to kinetic models of damage prediction.

Long-term moisture exposure at 95°C caused minimal permanent chemical damage, although it did cause a reversible hydrolysis reaction of imide rings. The  $T_g$  and  $T_{d5\%}$  of the neat polymer exhibited no change after 2000-h aging, demonstrating long-term hydrothermal stability. Furthermore, the  $T_g$  was largely unaffected by moisture exposure (in comparison to the dry  $T_g$  values), a finding attributed to the unusual stiffness of the polymer chains arisen by the asymmetric backbone structure, and effectively suppresses the plasticization effects of water molecules on  $T_g$ . Given the ~100% retention of  $T_g$  after hot/wet exposure, chain scissions appear to be absent or minimal in the reversible hydrolytic reactions.





Moisture exposure had a stronger effect on mechanical properties, although tensile modulus and strength exhibited little effect. Prior to long-term aging, moisture plasticization exhibited positive effects, increasing the ductility and toughness. However, ductility and toughness degradation arose after long-term hot/wet exposure. After 2000-h hydrothermal aging, the ductility decreased by 30-50%, resulting in a reduction in toughness of 30%-55%. The decrease in ductility and toughness was attributed to the long-term effects of hydrolysis and moisture plasticization. The mechanically active regions in the polymer network were consumed by moisture-induced chemical and physical reactions, evidenced by the decreased area of the  $\beta$ -transition in  $\tan \delta$  curves. The network structure change was irreversible, resulting in permanent mechanical degradation. The findings constitute a case study demonstrating use of  $\tan \delta$  to analyze structural change in polymer networks and resultant mechanical degradation upon physical/chemical aging. However, more investigation is required to establish more clearly the relationship between structural relaxations and mechanical behavior.

Although the ductility of the neat polymer decreased to 11.06% (dry) after 2000-h of aging, the retained ductility exceeded that of fresh conventional polyimides (e.g., 1.5% for dry PMR-15<sup>9</sup> and 2.41% for dry AFR-PE-4<sup>27</sup>). Moreover, after 1000-h of aging, continued exposure did not degrade the tensile properties further, and a steady state was achieved, indicating limited hydro-degradation on mechanical properties as aging time increased. In addition, after 2000-h aging, ~90% of the composite SBS strength was retained. The absence of thermal property deterioration, the negligible changes in chemical structure and the limited mechanical degradation, demonstrate promising stability for long-term performance in humid service conditions, and potential for long service life in hot-wet conditions.

## Acknowledgements

Please cite the article as: Zhang, Y., Miyauchi, M., & Nutt, S.. “**Moisture absorption and hydrothermal aging of phenylethynyl-terminated pyromellitic dianhydride-type asymmetric polyimide and composites,**” High Performance Polymers (2018), DOI: [10.1177/0954008318816754](https://doi.org/10.1177/0954008318816754)



The authors would like to thank William Guzman of Kaneka Americas Holding, Inc., and Mark Anders of University of Southern California (USC) for assistance with TriA X resin preparation and specimen machining, respectively. Thanks also go to Wei Hu of USC for guidance in data fitting.

## Declaration of conflicting interests

The author(s) declared no potential conflicts of interest with respect to the research, authorship, and/or publication of this article.

## Funding statement

The author(s) received no financial support for the research, authorship, and/or publication of this article.

## References

1. Kool G. Current and future materials in advanced gas turbine engines. *ASME 1994 International Gas Turbine and Aeroengine Congress and Exposition*, The Hague, Netherlands, June 13-16 1994.
2. Hergenrother P, Connell J, Smith Jr J. Phenylethynyl containing imide oligomers. *Polymer* 2000; **41**(13):5073-81.
3. Red C. The Outlook for Thermoplastics in Aerospace Composites, 2014-2023: *Composites World*; 2014 [Available from: <https://www.compositesworld.com/articles/the-outlook-for-thermoplastics-in-aerospace-composites-2014-2023>].
4. Hou T-H. Processing robustness for a phenylethynyl-terminated polyimide composite. *Journal of applied polymer science* 2006; **100**(4):3212-21.

Please cite the article as: Zhang, Y., Miyauchi, M., & Nutt, S.. “**Moisture absorption and hydrothermal aging of phenylethynyl-terminated pyromellitic dianhydride-type asymmetric polyimide and composites,**” *High Performance Polymers* (2018), DOI: **10.1177/0954008318816754**



5. Shin EE, Morgan RJ, Zhou J. Hydrolytic degradation mechanisms and kinetics of polyimides for advanced composites. *Society for the advancement of material and process engineering conference proceedings*, Long Beach, CA, 21-25 May 2000.
6. Shin EE, Morgan RJ, Zhou J, Lincoln J, Jurek R, Curliss DB. Hygrothermal durability and thermal aging behavior prediction of high-temperature polymer-matrix composites and their resins. *Journal of Thermoplastic Composite Materials* 2000; **13**(1):40-57.
7. Bao L-R, Yee AF, Lee CY-C. Moisture absorption and hygrothermal aging in a bismaleimide resin. *polymer* 2001; **42**(17):7327-33.
8. Cowie JMG, Arrighi V *Polymers: chemistry and physics of modern materials*. Boca Raton, FL, USA: CRC press, 2007.
9. *CYCOM® 2237 polyimide resin system*. Woodland Park, NJ: Cytec Solvay Group, 2012.
10. Serafini T, Hanson M. Environmental effects on graphite fiber reinforced PMR-15 polyimide. *Composites for Extreme Environments*. West Conshohocken, PA: ASTM International, 1982.
11. Burcham LJ, Vanlandingham MR, Eduljee RF, Gillespie Jr JW. Moisture effects on the behavior of graphite/polyimide composites. *Polymer composites* 1996; **17**(5):682-90.
12. Han M-H, Nairn JA. Hygrothermal aging of polyimide matrix composite laminates. *Composites Part A: Applied science and manufacturing* 2003; **34**(10):979-86.
13. Czabaj MW, Zehnder AT, Chuang KC. Blistering of moisture saturated graphite/polyimide composites due to rapid heating. *Journal of Composite Materials* 2009; **43**(2):153-74.
14. Fang X, Rogers DF, Scola DA, Stevens M. A study of the thermal cure of a phenylethynyl-terminated imide model compound and a phenylethynyl-terminated imide oligomer (PETI-5). *Journal of Polymer Science Part A: Polymer Chemistry* 1998; **36**(3):461-70.

Please cite the article as: Zhang, Y., Miyauchi, M., & Nutt, S.. “**Moisture absorption and hydrothermal aging of phenylethynyl-terminated pyromellitic dianhydride-type asymmetric polyimide and composites**,” *High Performance Polymers* (2018), DOI: **10.1177/0954008318816754**



15. Fang X, Xie X-Q, Simone CD, Stevens MP, Scola DA. A solid-state  $^{13}\text{C}$  NMR study of the cure of  $^{13}\text{C}$ -labeled phenylethynyl end-capped polyimides. *Macromolecules* 2000; **33**(5):1671-81.
16. Zhang Y, Jain A, Grunenfelder LK, Miyauchi M, Nutt S. Process development for phenylethynyl-terminated PMDA-type asymmetric polyimide composites. *High Performance Polymers* 2018; **30**(6):731-41.
17. Zhang Y, Miyauchi M, Nutt S. Structure and properties of a phenylethynyl-terminated PMDA-type asymmetric polyimide. *High Performance Polymers* 2018. DOI: 10.1177/0954008318762592.
18. Greenspan L. Humidity fixed points of binary saturated aqueous solutions. *Journal of research of the national bureau of standards* 1977; **81**(1):89-96.
19. ASTM D638-14. *Standard Test Method for Tensile Properties of Plastics*. West Conshohocken, PA: ASTM International, 2014.
20. ASTM D2344. *Standard test method for short-beam strength of polymer matrix composite materials and their laminates*. West Conshohocken, PA: ASTM International, 2016.
21. Shen C-H, Springer GS. Moisture absorption and desorption of composite materials. *Journal of composite materials* 1976; **10**(1):2-20.
22. El-Sa'ad L, Darby M, Yates B. Moisture absorption by epoxy resins: the reverse thermal effect. *Journal of Materials Science* 1990; **25**(8):3577-82.
23. Bao L-R, Yee AF. Effect of temperature on moisture absorption in a bismaleimide resin and its carbon fiber composites. *Polymer* 2002; **43**(14):3987-97.
24. Bower DI *An introduction to polymer physics*. New York, NY, USA: Cambridge University Press, 2002. pp. 212-213.

Please cite the article as: Zhang, Y., Miyauchi, M., & Nutt, S.. “**Moisture absorption and hydrothermal aging of phenylethynyl-terminated pyromellitic dianhydride-type asymmetric polyimide and composites,**” *High Performance Polymers* (2018), DOI: **10.1177/0954008318816754**



25. Mikols W, Seferis J, Apicella A, Nicolais L. Evaluation of structural changes in epoxy systems by moisture sorption-desorption and dynamic mechanical studies. *Polymer Composites* 1982; **3**(3):118-24.
26. Yu Q, Zhou M, Ding Y, Jiang B, Zhu S. Development of networks in atom transfer radical polymerization of dimethacrylates. *Polymer* 2007; **48**(24):7058-64.
27. Lincoln JE (2001). *Structure-property-processing relationships and the effects of physical structure on the hygrothermal durability and mechanical response of polyimides*. PhD Thesis, Michigan State University, USA.
28. Immergut EH, Mark HF. Principles of Plasticization. *Plasticization and Plasticizer Processes*. Advances in Chemistry. 48. Washington, DC, USA: American Chemical Society, 1965. p. 1-26.
29. Johari G. Localized molecular motions of  $\beta$ -relaxation and its energy landscape. *Journal of non-crystalline solids* 2002; **307**:317-25.
30. Bao L-R, Yee AF. Moisture diffusion and hygrothermal aging in bismaleimide matrix carbon fiber composites—part I: uni-weave composites. *Composites Science and Technology* 2002; **62**(16):2099-110.
31. Ahmed KS, Vijayarangan S. Tensile, flexural and interlaminar shear properties of woven jute and jute-glass fabric reinforced polyester composites. *Journal of materials processing technology* 2008; **207**(1-3):330-5.
32. Tompkins S, Williams SL. Effects of thermal cycling on mechanical properties of graphite polyimide. *Journal of Spacecraft and Rockets* 1984; **21**(3):274-80.



Please cite the article as: Zhang, Y., Miyauchi, M., & Nutt, S.. **“Moisture absorption and hydrothermal aging of phenylethynyl-terminated pyromellitic dianhydride-type asymmetric polyimide and composites,”** High Performance Polymers (2018), DOI: [10.1177/0954008318816754](https://doi.org/10.1177/0954008318816754)